



Cite this: DOI: 10.1039/c4ob02528h

## A comparison of chemiluminescent acridinium dimethylphenyl ester labels with different conjugation sites†

Anand Natrajan\* and David Wen

Chemiluminescent acridinium dimethylphenyl esters are highly sensitive labels that are used in automated assays for clinical diagnosis. Light emission from these labels and their conjugates is triggered by treatment with alkaline peroxide. Conjugation of acridinium ester labels is normally done at the phenol. During the chemiluminescent reaction of these acridinium esters, the phenolic ester is cleaved and the light emitting acridone moiety is liberated from its conjugate partner. In the current study, we report the synthesis of three new acridinium esters with conjugation sites at the acridinium nitrogen and compare their properties with that of a conventional acridinium ester with a conjugation site at the phenol. Our study is the first that provides a direct comparison of the emissive properties of acridinium dimethylphenyl esters (free labels and protein conjugates) with different conjugation sites, one where the light emitting acridone remains attached to its conjugate partner *versus* conventional labeling which results in cleavage of the acridone from the conjugate. Our results indicate that the conjugation at the acridinium nitrogen, which also alters how the acridinium ring and phenol are oriented with respect to the protein surface, has a minimal impact on emission kinetics and emission spectra. However, this mode of conjugation to three different proteins led to a significant increase in light yield which should be useful for improving the assay sensitivity.

Received 2nd December 2014,  
Accepted 2nd January 2015

DOI: 10.1039/c4ob02528h

www.rsc.org/obc

## Introduction

Chemiluminescent acridinium dimethylphenyl esters<sup>1</sup> are highly sensitive labels that are used in automated immunoassays for clinical diagnosis. Conjugates of these labels are used along with magnetic microparticles for the measurement of a wide range of clinically important analytes.<sup>1a–d</sup> Light emission from acridinium ester labels and their conjugates is typically triggered with alkaline peroxide. Acridinium esters at physiological pH exist as non-chemiluminescent water adducts (commonly referred to as pseudobases<sup>1g,h,2</sup>) that are formed by the addition of water at C-9 of the acridinium ring (see Fig. 1 for the numbering system). Consequently, an acid pre-treatment is required to convert the pseudobases to the acridinium forms before the chemiluminescence can be initiated from acridinium ester labels and their conjugates. In practice, at the end of each immunoassay on our automated instruments, chemiluminescence is triggered by the sequential addition of 0.1 M

nitric acid containing 0.5% hydrogen peroxide followed by the addition of 0.25 M sodium hydroxide containing the cationic surfactant cetyltrimethylammonium chloride (CTAC).<sup>1e</sup> The surfactant accelerates light emission from the labels by providing a high local concentration of reactive hydroperoxide ions at the cationic micellar surface.<sup>1e</sup> Micelles of CTAC also provide a low-polarity environment<sup>1e,3</sup> which is conducive to the formation of dioxetanes and/or dioxetanones that have been proposed as reaction intermediates in the chemiluminescence pathway of acridinium esters.<sup>4</sup> Ultimately, excited state acridone is believed to be the light emitting moiety responsible for the acridinium ester chemiluminescence.<sup>4</sup>

Conjugation of acridinium esters to biomolecules such as proteins can potentially be carried out at different sites of the acridinium ester molecule as illustrated in Fig. 1, panel A. For immunoassay applications, conjugation of acridinium dimethylphenyl ester labels is typically carried out at the phenol by placement of a reactive group as illustrated in structure 4, which has an *N*-hydroxysuccinimide active ester appended to a polar, zwitterion-containing linker (Fig. 1, panel B).<sup>1g</sup> In fact, conjugation at the phenol is the most commonly described strategy in the literature for applications in immunoassays as well as probe assays.<sup>1,5</sup> This is because of two

Siemens Healthcare Diagnostics, Advanced Technology and Pre-Development, 333 Coney Street, East Walpole, MA 02032, USA. E-mail: anand.natrajan@siemens.com; Fax: +1-508-660-4591; Tel: +1-508-660-4582

† Electronic supplementary information (ESI) available. See DOI: 10.1039/c4ob02528h

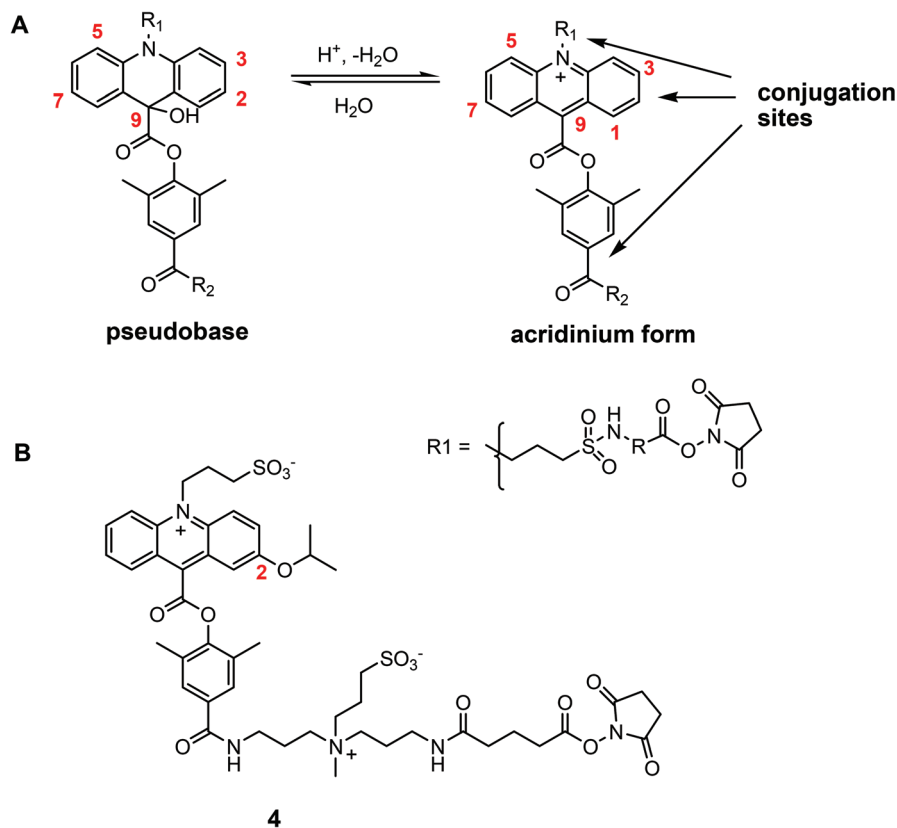


**Fig. 1** Panel A: general structure of a chemiluminescent acridinium dimethylphenyl ester illustrating pseudobase-acridinium equilibrium. Potential sites for conjugation are indicated by the arrows. In the current study, conjugation sites were incorporated at R1 at the acridinium nitrogen using sulfonylpentafluorophenyl chemistry.<sup>1h</sup> Panel B: structure of a high light yield, *N*-sulfopropyl acridinium dimethylphenyl ester with a C-2 isopropoxy group and a hydrophilic, zwitterionic linker containing a conjugation site attached to the phenol.<sup>1g</sup>

main reasons. First, incorporating a conjugation site at the phenol is relatively easy from a synthesis point of view. In addition, this approach leaves the acridinium ring intact for suitable chemical modification to both alter the emissive properties of the label and influence its partitioning into CTAC micelles. For example in structure **4** (Fig. 1, panel B), the isopropoxy group at C-2 of the acridinium ring not only induces a bathochromic shift in the emission wavelength but also increases the light yield twofold compared to the corresponding unsubstituted label.<sup>1g</sup> Moreover, the isopropoxy group increases the hydrophobicity of the acridinium ring which results in its strong partitioning into CTAC micelles.<sup>1g</sup> The other reason why acridinium ester conjugation is typically carried out at the phenol is because during light emission, the phenolic ester is cleaved and the light emitting acridone moiety is free to diffuse away from its conjugate partner such as a protein as illustrated in Fig. 2, panel B. Thus, the impact of the protein on chemiluminescence is expected to be minimal. On the other hand if conjugation is carried out either at the acridinium nitrogen (illustrated in Fig. 2, panel A) or at other sites on the acridinium ring, then following the chemiluminescence reaction, the light emitting acridone will remain attached to the protein and its chemiluminescence can be potentially affected.

Conjugation of acridinium esters to various molecules, either at the acridinium ring carbons or at the acridinium nitrogen (Fig. 1, panel A), is synthetically more challenging but has also been described in the literature.<sup>6</sup> For example, syntheses of conjugates of acridinium dimethylphenyl esters to various fluorescent dyes linked either through the acridinium ring at C-2/C-3 or the acridinium nitrogen have been described.<sup>6a</sup> These conjugates showed very efficient energy transfer from excited state acridone to the attached dye when their chemiluminescence is triggered with alkaline peroxide. A range of chemiluminescent, acridinium ester conjugates of fluorescent dyes emitting at different wavelengths was described using this strategy.<sup>6a</sup> Acridinium dimethylphenyl ester labels with conjugation sites at C-2 have also been shown to be potentially useful for homogeneous immunoassays using resonance energy transfer.<sup>6b</sup>

Synthetic access to acridinium esters with conjugation sites at C-2 or C-3, although somewhat tedious, is relatively straightforward but functionalization of the acridine nitrogen with complex alkylating reagents is much more difficult due to steric hindrance. Conjugation through the acridinium nitrogen, nevertheless, is attractive because it leaves C-2 and C-3 in the acridinium ring free for modification with other functional groups such as in **4** (Fig. 1). Functionalization of the acridine

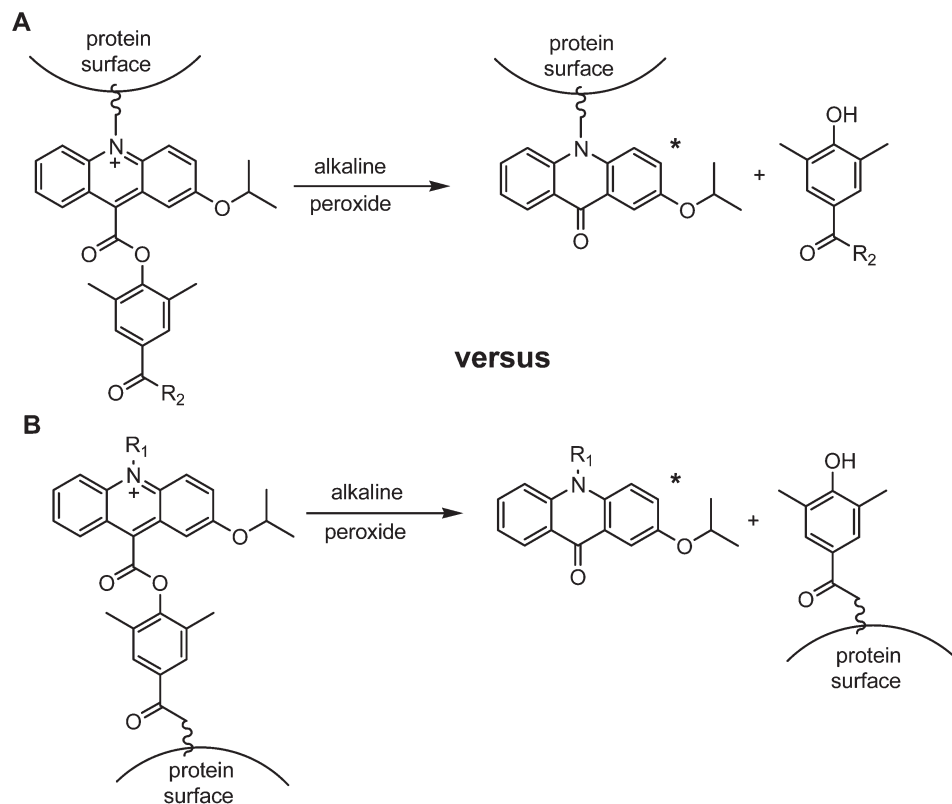


**Fig. 2** Fate of the light-emitting, acridone moiety following chemiluminescent reaction of a protein conjugate of an acridinium dimethylphenyl ester. Panel A: when conjugation is performed at the acridinium ring (illustrated for the acridinium nitrogen) the light emitting acridone species remains attached to the protein. Panel B: when conjugation is performed at the phenol, excited state acridone is cleaved from the protein and can diffuse away from the protein surface.

nitrogen in variable yields has been described in the literature using reagents such as *tert*-butyl iodoacetate or other simple alkyl iodides and bromides as both the alkylating reagent and solvent.<sup>7a,b</sup> N-Alkylation of the acridine nitrogen in acridine esters and related compounds with powerful trifluoromethanesulfonates (triflates) as alkylating reagents has been reported to afford better yields in a few instances<sup>8</sup> although in more recent studies,<sup>9</sup> reported yields were quite poor for these N-alkylation reactions even with very reactive alkylating reagents. Consistent with these later studies,<sup>9</sup> in our experience, with the exception of strong methylating reagents or 1,3-propane sultone,<sup>1</sup> the N-alkylation of acridine dimethylphenyl ester precursors is very difficult to achieve in good yields even with powerful alkylating reagents such as trifluoromethanesulfonates. On the other hand, introduction of the *N*-sulfopropyl group can be conveniently carried out in a wide range of acridine dimethylphenyl ester substrates in excellent yields by using room temperature ionic liquids as reaction media and using commercially available 1,3-propane sultone as the alkylating reagent.<sup>1f-j,10</sup>

We reported recently that the *N*-sulfopropyl group in a 2-isopropoxy-substituted acridinium ester can easily be converted to the activated but stable sulfonyl pentafluorophenyl ester *via* the sulfonyl chloride.<sup>1h</sup> We used this pentafluorophenyl ester to

assemble a hydrophilic, charge-neutral acridinium ester which exhibited high light yield and low non-specific binding to magnetic microparticles.<sup>1h</sup> In the current study, we report the synthesis of three new acridinium esters with conjugation sites at the acridinium nitrogen using *N*-sulfonyl pentafluorophenyl ester chemistry and our simple synthetic protocol should prove useful for the assembly of other acridinium esters with complex *N*-alkyl functional groups. We provide a comparison of these new acridinium esters and their protein conjugates to three different proteins with different isoelectric points (pI), with a structurally analogous acridinium ester **4** which has a conjugation site at the phenol. Our study is the first that provides a direct comparison of the properties of acridinium dimethylphenyl esters (free labels and protein conjugates) with different conjugation sites. Conjugation at the acridinium nitrogen reverses the orientation of the acridinium ring and phenol with respect to the protein surface compared to labeling at the phenol (Fig. 2). In addition, in the former, the light emitting acridone moiety remains attached to its conjugate partner *versus* conventional labeling which results in cleavage of the acridone from the conjugate. Our results provide insight into the contributions of the microenvironment of the cationic surfactant CTAC and proteins in affecting the acridinium ester chemiluminescence.

## Results and discussion

### Synthesis of acridinium esters and conjugates

The synthesis of three acridinium dimethylphenyl esters **3a–3c** containing a C-2 isopropoxy group and with three different linkers attached to the acridinium nitrogen is illustrated in Fig. 3. The syntheses were accomplished using the common intermediate **1** whose synthesis we have described recently.<sup>1h</sup> The synthesis of **1** is straightforward and entails conversion of

the sulfonate moiety in the *N*-sulfopropyl acridinium ester to the acid chloride using thionyl chloride followed by condensation with pentafluorophenol. Compared to the sulfonyl chloride, the sulfonyl pentafluorophenyl ester **1** is much more stable. It can conveniently be purified by preparative HPLC (if required) and is stable to storage under anhydrous conditions at low temperatures ( $\sim -10$  °C) for an extended period of time (months).

We wanted to determine whether the length and nature of the linker attached to the acridinium nitrogen would affect its

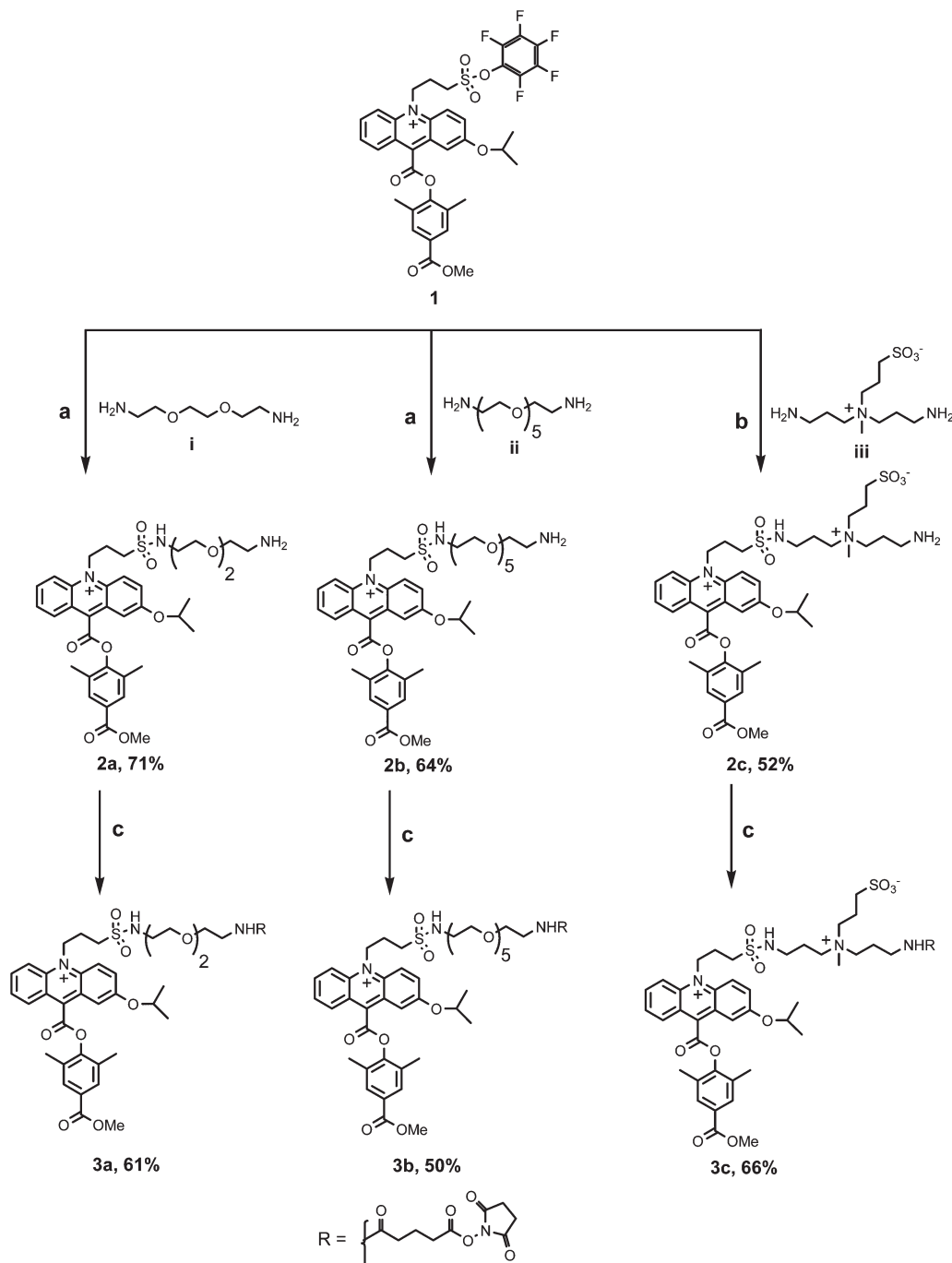


**Fig. 3** Synthetic scheme for compounds **3a–3c** with conjugation sites at the acridinium nitrogen. (a) **1** : **1**, DMF–MeCN, 75 °C; (b) DMSO, diisopropylethylamine (DIPEA) 75 °C; (c) disuccinimidyl glutarate (DSG), 0.1 M sodium phosphate pH = 7.2/MeCN.

**Table 1** Label incorporation in proteins using 10 equivalents input of acridinium ester labels **3a–3c** and **4** in the labeling reactions. Label incorporation (rounded to the nearest integer) was measured by mass spectroscopy

Label	BSA	Anti-TSH Mab	Anti-HBsAg Mab
<b>4</b>	6.0	6.0	8.0
<b>3a</b>	5.0	4.0	3.0
<b>3b</b>	4.0	4.0	6.0
<b>3c</b>	7.0	8.0	6.0

chemiluminescence. In addition, we wanted to maintain adequate aqueous solubility of the acridinium esters. Towards that end, three different linkers, two **i** and **ii** derived from poly(ethylene)glycol and one **iii** containing a sulfobetaine zwitterion were selected for reaction with **1**. Linker **i** is commercially available and we have reported the syntheses of **ii** and **iii** in our earlier work.<sup>1b,e</sup> Displacement of the pentafluorophenyl ester in **1** by **i–iii** was easily accomplished by heating **1** with a 5-fold excess of the three linkers to give the amine derivatives **2a–2c**. These displacement reactions proceeded cleanly with minimal hydrolysis of the pentafluorophenyl ester **1**. Following HPLC purification of **2a–2c**, they were converted to the *N*-hydroxysuccinimide esters **3a–3c** using standard chemistry followed by HPLC purification. Yields of all compounds following HPLC purification were generally quite good as detailed in the Experimental section and in Fig. 3. HPLC traces and NMR spectra of compounds **2a–2c** and **3a–3c** are shown in Fig. S1–S6 (ESI†).

Protein conjugates were prepared using labels **3a–3c** and **4**, the latter representing a conventional acridinium ester with the same C-2 isopropoxy group but with the conjugation site at the phenol as described earlier. Three different proteins were selected, BSA (BSA = bovine serum albumin, a small acidic protein), an anti-TSH monoclonal antibody<sup>1e</sup> (Mab) with an acidic pI of 5.6 (TSH = thyroid stimulating hormone) and an anti-HBsAg Mab<sup>1e</sup> with a neutral pI of 6.9 (HBsAg = hepatitis B surface antigen). Label incorporation in these three different proteins (Table 1) was measured by mass spectroscopy. Some differences were noted in the labeling efficiency between the four labels with **3a** and **3b** leading to slightly lower levels of incorporation compared to **4** and **3c** which have more polar, zwitterion-containing linkers. For a given acridinium ester however, label incorporation across the three different proteins was quite similar. For example **3c** gave 7, 8 and 6 incorporated labels respectively in BSA, anti-TSH Mab and anti-HBsAg Mab. Thus, protein pI did not play a significant role in labeling efficacy for a particular label.

### Chemiluminescence measurements

Chemiluminescence measurements of the free labels, amine derivatives **2a–2c** as well as the amine precursor<sup>1g</sup> of **4** were carried out using a luminometer and a spectral camera as described in the Experimental section. (The amine derivatives **2a–2c** were used to avoid hydrolysis of the *N*-hydroxysuccinimide esters that are appended to the zwitterionic linker in the

corresponding labels **3a–3c** and **4**). Similarly, protein conjugates of the labels **3a–3c** and **4** were used for chemiluminescence measurements. Both the free labels as well as the protein conjugates were also used for recording emission spectra. The output of the luminometer was in RLUs (Relative Light Units) whereas emission spectra recorded using the spectral camera had an output of emission intensity (luminescence) as a function of emission wavelength.

For chemiluminescence measurements of the free labels, the amine derivatives **2a–2c** (precursors to the NHS esters **3a–3c**) and the amine precursor of **4** were dissolved in dimethyl sulfoxide (0.25–0.5 mM) and these solutions were serially diluted to 0.25–0.5 nM concentrations in buffer. Chemiluminescence from 0.01 mL samples was initiated by the addition of 0.3 mL of 0.1 M nitric acid containing 0.5% hydrogen peroxide followed by the instantaneous addition of 0.25 M sodium hydroxide with or without CTAC (7 mM). In the presence of CTAC, emission was fast (similar to what we have reported previously<sup>1e</sup>) and light was collected for a period of 10 seconds integrated at 0.1 second intervals (five replicates). In the absence of CTAC, light emission from acridinium dimethylphenyl esters is typically slow<sup>1e</sup> and therefore light was collected for a period of 2 minutes integrated at 0.5 second intervals. Chemiluminescence measurements of protein conjugates were carried out in a similar manner. Protein conjugates (~2 mg mL<sup>-1</sup>) were serially diluted to 0.1–0.2 nM and the chemiluminescence from 0.01 mL samples was measured as described above. Additional details can be found in the Experimental section.

Chemiluminescence emission profiles in the presence of CTAC of the free labels **2a–2c**, the amine precursor of **4** as well as the three protein conjugates of the four labels **3a–3c** and **4** are shown in Fig. 4. The corresponding emission profiles in the absence of CTAC are also shown in Fig. S7–S10 (ESI†). As can be noted from Fig. 4, both the free labels as well as the protein conjugates of the various labels exhibited fast light emission in the presence of CTAC with total emission times of <5 seconds regardless of the label or the protein. This fast emission is typical of acridinium dimethylphenyl esters<sup>1e</sup> and the emission profiles illustrated in Fig. 4 indicate that the conjugation site does not play any significant role in emission kinetics. The fast light emission also implies that the acridinium rings in the various labels as well as in their conjugates are able to partition equally well into CTAC micelles which are responsible for accelerating light emission.<sup>1e</sup> In the absence of CTAC, light emission from the free labels as well as the protein conjugates was slow, taking up to a minute for complete emission as illustrated in Fig. S7–S10 (ESI†).

Emission spectra of the labels and protein conjugates are shown in Fig. 5 and S11 and S12 (ESI†). For compound **4**, the conjugation site is at the phenol and the acridone is released during the chemiluminescence reaction following cleavage of the phenolic ester bond. Consequently, any change in the emission spectrum of the acridone is unlikely for the conjugate and Fig. 5 (panel A) confirms this expectation. Both the free label and the BSA conjugate showed emission from the

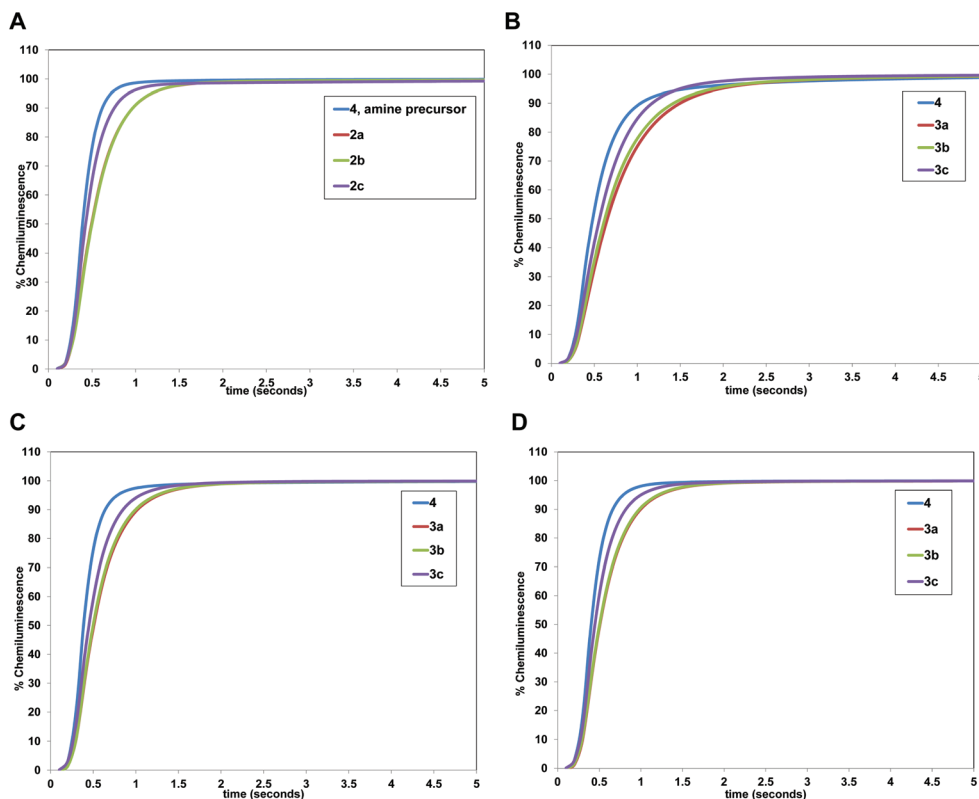


**Fig. 4** Chemiluminescence emission profiles. Panel A: free labels, the amine precursor of **4** and amine precursors **2a–2c**. Panel B: BSA conjugates of compound **4** and **3a–3c**. Panel C: anti-TSH Mab conjugates of compound **4** and **3a–3c**. Panel D: anti-HBsAg Mab conjugates of compound **4** and **3a–3c**. Chemiluminescence was initiated by the sequential addition of 0.3 mL of 0.1 M nitric acid containing 0.5% hydrogen peroxide followed by 0.3 mL of 0.25 M sodium hydroxide containing 7 mM CTAC (CTAC = cetyltrimethylammonium chloride). Fast light emission was observed regardless of the conjugation site for both free labels and protein conjugates.

2-isopropoxy-substituted acridone<sup>1h</sup> with an emission maximum centered at 452–454 nm. For the free labels **2a–2c**, the same 2-isopropoxy-substituted acridone is formed in the reaction although with different *N*-alkyl groups. All three labels **2a–2c** showed identical emission spectra compared to the amine precursor of **4** with emission maxima centered at 454 nm. These results are consistent with our earlier study where we noted that the structure of the *N*-alkyl group in a 2-isopropoxy-substituted, charge-neutral acridinium ester had no impact on its emission spectrum.<sup>1h</sup> The BSA conjugates of the labels **3a–3c** interestingly also showed very similar emission spectra to the free labels (Fig. 5, panels B–D). These observations indicate that even when the light emitting acridone moieties from these labels are constrained on the protein, their emission spectra are largely unaffected. Similarly, the antibody conjugates of **4** and **3a–3c** showed identical emission spectra regardless of the conjugation site as illustrated in Fig. S11 and S12 (ESI†).

Is the light yield affected when conjugation of acridinium dimethylphenyl esters is performed using functional groups at the acridinium nitrogen rather than at the phenol? To answer this question, we measured the specific chemiluminescence activity of the free labels as well their protein conjugates (both with and without CTAC) and the results are shown in Fig. 6

(with CTAC). For label **4** with a conjugation site at the phenol, the specific activity was observed to be relatively unchanged from the free label to its protein conjugates. Thus the specific activity of the free label was observed to be 5.4 (units of  $10^{19}$  RLUs per mole) whereas the corresponding values were 5.3, 5.1 and 4.4 for BSA, anti-TSH Mab and anti-HBsAg Mab conjugates, respectively. In comparison, the free labels **2a–2c** showed a slight drop in specific activity when compared to **4** as shown in Fig. 6. However unlike **4**, conjugation of the NHS esters **3a–3c** (corresponding to the amine derivatives **2a–2c**) to the three proteins showed a consistent increase in light yield compared to the free labels as can be noted from Fig. 6. These observations may appear counterintuitive because the excited state acridone moieties from **3a–3c** are constrained on the proteins and could potentially be subjected to quenching by the latter's aromatic amino acids. However, all three labels emit light with wavelength maxima at 454 nm which is well separated from the dominant absorption band of BSA and antibodies at 280 nm. Consequently quenching by energy transfer is expected to be unlikely which is consistent with our observations.

To better understand the mechanism of the enhancement in light yield for the protein conjugates of **3a–3c**, we calculated the relative change in light yield caused by protein conjugation



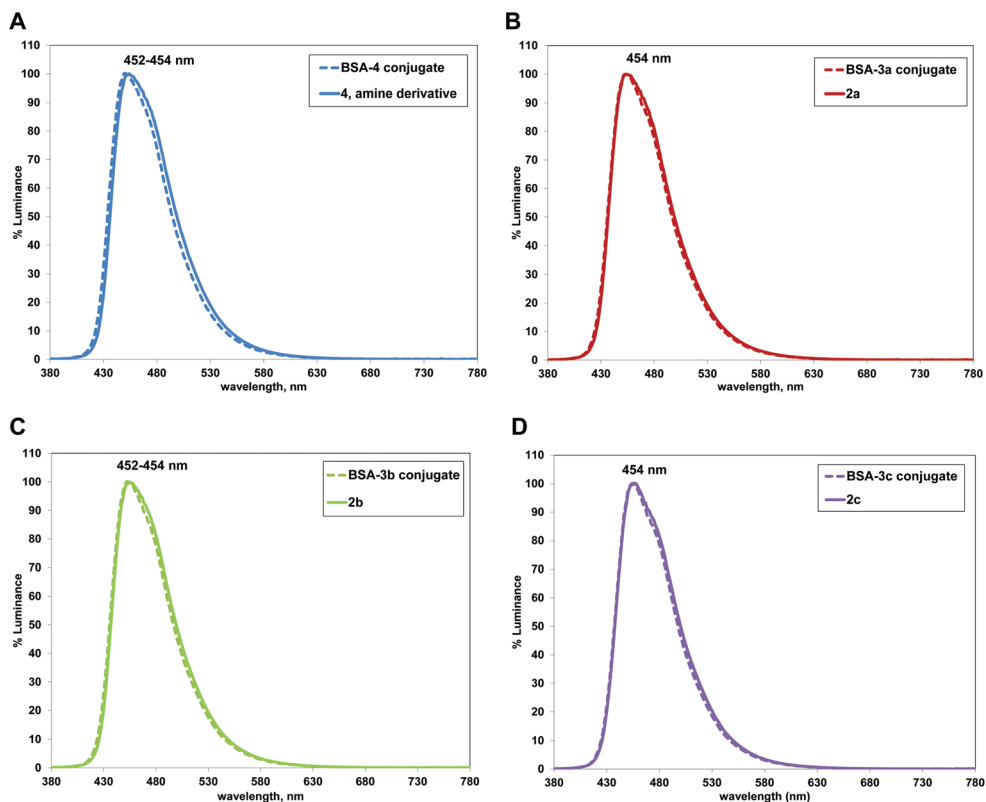


**Fig. 5** Emission spectra. Panel A: **4** (amine precursor) and the BSA conjugate of **4**. Panel B: **2a** and the BSA conjugate of **3a**. Panel C: **2b** and the BSA conjugate of **3b**. Panel D: **2c** and the BSA conjugate of **3c**. Emission spectra were obtained on an FSSS (Fast Spectral Scanning System) using a PR-740 spectroradiometer (camera) from Photo Research Inc. Emission spectra of acridinium esters and BSA conjugates did not change regardless of the conjugation site and even when excited state acridones from **3a–3c** were constrained on the protein.

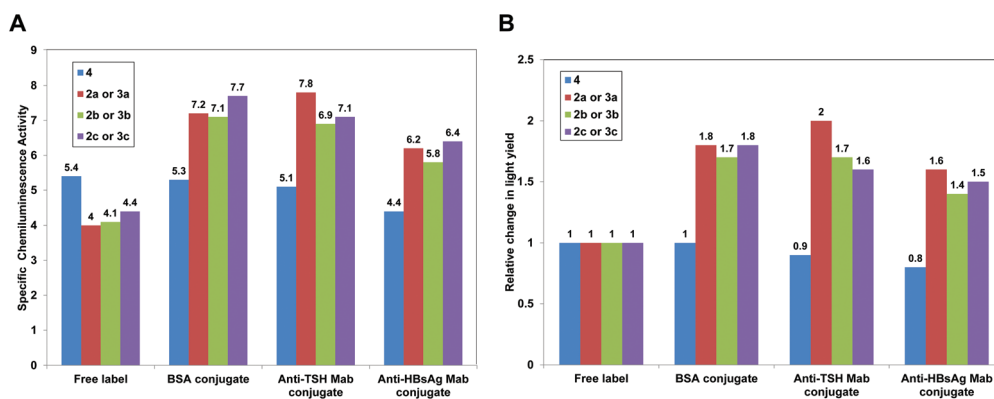


**Fig. 6** Panel A: observed specific chemiluminescence activity (SCA) in units of  $10^{19}$  RLU per mole of acridinium ester labels and their protein conjugates (average of five replicates). Panel B: relative change in the light yield caused by protein conjugation. Specific activities of the free labels (amine precursor of **4** and **2a–2c**) were assigned a value of one. Conjugation of the labels **3a–3c** (NHS esters corresponding to **2a–2c**) through conjugation sites at the acridinium nitrogen led to an increase in the light yield in the protein conjugates. A corresponding increase was not observed when conjugation was performed at the phenol for **4**.

(free labels *versus* conjugates) as illustrated in Fig. 6, panel B. In panel B, the specific activity of each free label (**2a–2c** and amine derivative of **4**) was assigned a value of one. In addition, in Table 2, we have listed the observed enhancements in light yields for the free labels and the protein conjugates in the presence of CTAC compared to the control experiments

without CTAC. Table 2 also lists the ratios of the enhancements in light yield caused by CTAC for conjugates *versus* free labels.

An examination of Fig. 6 and Table 2 reveals some interesting differences between the different labels and their protein conjugates while at the same time illustrating the complexity

**Table 2** Observed enhancement (fold) in the chemiluminescence of free labels and protein conjugates in the presence of CTAC. Light emission was triggered by the sequential addition of 0.3 mL of 0.1 M nitric acid containing 0.5% hydrogen peroxide followed by 0.25 M sodium hydroxide with or without CTAC (control experiment). The light yield in the absence of the surfactant was assigned a value of one for each label and conjugate. Values in parentheses are the ratios in CTAC enhancements of conjugates *versus* free labels (assigned a relative value of one)

Free label/conjugate	CTAC enhancement, (conjugate/free label)
4, amine precursor <sup>1g</sup>	4.1
2a	4.3
2b	3.7
2c	4.3
BSA-4	3.7 (0.9)
BSA-3a	4.8 (1.1)
BSA-3b	4.5 (1.2)
BSA-3c	4.0 (0.9)
anti-TSH Mab-4	4.6 (1.1)
anti-TSH Mab-3a	5.9 (1.4)
anti-TSH Mab-3b	5.4 (1.5)
anti-TSH Mab-3c	6.2 (1.4)
anti-HBsAg Mab-4	6.1 (1.5)
anti-HBsAg Mab-3a	6.1 (1.4)
anti-HBsAg Mab-3b	5.0 (1.4)
anti-HBsAg Mab-3c	5.9 (1.4)

of the effects leading to these observed differences. For label 4, which has the conjugation site at the phenol, the overall light yield was observed to be minimally affected by conjugation to three different proteins (Fig. 6). The observed enhancements in light yield caused by CTAC for 4 and its protein conjugates were also quite similar except for the neutral anti-HBsAg antibody as can be noted in Table 2. For example, CTAC enhancements in the chemiluminescence of the free label 4 compared to its BSA, anti-TSH Mab and anti-HBsAg Mab conjugates were observed to be 4.1, 3.7, 4.6 and 6.1, respectively.

For labels 3a–3c with conjugation sites at the acridinium nitrogen, unlike for 4, a significant increase in light yield was observed upon protein conjugation (Fig. 6). For example for 3a, conjugation to BSA, anti-TSH and anti-HBsAg antibodies was observed to result in an increase in light yield of 1.8, 2.0 and 1.6-fold respectively compared to the free label (Fig. 6). Similar increases were noted for labels 3b and 3c. Is this increase in light yield in the protein conjugates of 3a–3c due to greater surfactant-mediated enhancement? The enhancements in light yields for 2a/3a and its protein conjugates caused by CTAC were observed to be 4.3, 4.8, 5.9 and 6.1-fold for the free label *versus* its BSA, anti-TSH and anti-HBsAg antibody conjugates, respectively. Thus, even though a large increase (1.8-fold) in light yield was observed for the BSA conjugate of 3a (Fig. 6), this increase cannot be attributed solely to greater CTAC enhancement in the conjugate *versus* the free label (1.1-fold, Table 2). Similarly, although greater CTAC enhancements were observed for the anti-TSH and anti-HBsAg antibody conjugates of 3a, the magnitude of these enhancements (1.4-fold) are not sufficient to explain the observed increases (2.0-fold for anti-TSH Mab and 1.6-fold for anti-HBsAg Mab) in light yields in Fig. 6 based solely on

different surfactant-mediated enhancements in conjugates *versus* free labels. Similar arguments apply for 3b and 3c. Thus, an increased light yield from the protein conjugates of 3a–3c appears to be due to a combination of two factors: (a) intrinsically higher light yield in the conjugates in the absence of CTAC especially for the BSA conjugates, and (b) greater CTAC enhancement in the light yield for the antibody conjugates.

In our earlier work,<sup>1e</sup> we proposed that surfactant-mediated enhancements in the light yield of acridinium dimethylphenyl esters and their conjugates result from the less polar micellar environment which is conducive to the formation of the immediate precursors (dioxetane and/or dioxetanone) of excited state acridone. Obviously, this requires strong partitioning of the acridinium ring into surfactant micelles and we provided evidence that this partitioning results from a combination of hydrophobic and charge interactions.<sup>1g</sup> Our current results indicate that acridinium dimethylphenyl esters with conjugation sites at the acridinium nitrogen and their protein conjugates are also equally capable of partitioning into surfactant aggregates. In addition to the micellar environment, the environment of the protein also appears to play a role in affecting the light yield from these labels compared to conventional acridinium ester labels with conjugation sites at the phenol. The combined environment of the protein and CTAC experienced by labels 3a–3c appears to be less polar based on the observed increases in the light yields for the conjugates. BSA in particular is known to bind a variety of ligands<sup>11</sup> and acridinium ester conjugation at the acridinium nitrogen places the acridinium ring closer to the protein surface and more susceptible to solubilization in less polar regions of the protein. Because the fluorescence quantum yield of acridones actually decreases with decreasing solvent polarity,<sup>1e,12</sup> the mechanism of light enhancement for the protein conjugates of 3a–3c must also involve facile formation of dioxetane/dioxetanone precursors in the combined micellar/protein microenvironment and not because excited state acridone is constrained in a less polar environment on the protein.

Besides the increased specific activity, the increased stability of chemiluminescent acridinium esters is another useful property for applications in commercial assays. Poor stability can compromise assay sensitivity and decrease reagent shelf life. The acridinium esters 3a–3c showed increased light output when conjugated to proteins which is very attractive for improving the immunoassay sensitivity. We also compared the chemiluminescence stability of the BSA conjugates of these labels with that of the conventional label 4 at two different pH values and the results are shown in Tables 3 and 4. As can be noted from these tables, BSA conjugates of 3a–3c were observed to be equally stable as the conjugate of 4 at both pH = 6 and 7.4 showing only a small drop of approximately 10% in activity after 30 days at room temperature. Reagents on automated instruments such as the ADVIA Centaur® systems are kept refrigerated so the loss of chemiluminescence under these conditions is expected to be minimal based on the stability data at room temperature.



**Table 3** Percent residual chemiluminescence (average of five replicates) of BSA conjugates of **3a–3c** and **4** in phosphate buffer, pH 6 at 25 °C. (CV = coefficient of variation of measurements)

Day	<b>4</b> (%CV)	<b>3a</b> (%CV)	<b>3b</b> (%CV)	<b>3c</b> (%CV)
1	100 (0.3)	100 (2.6)	100 (2.8)	100 (4.8)
8	100 (2.3)	100 (2.5)	101 (1.8)	99 (3.9)
17	98 (3.2)	99 (2.1)	98 (2.2)	98 (6.5)
23	94 (2.8)	94 (1.1)	92 (0.3)	91 (4.5)
30	88 (1.2)	90 (0.9)	93 (2.4)	87 (3.3)

**Table 4** Percent residual chemiluminescence (average of five replicates) of BSA conjugates of **3a–3c** and **4** in phosphate buffer, pH 7.4 at 25 °C

Day	<b>4</b> (%CV)	<b>3a</b> (%CV)	<b>3b</b> (%CV)	<b>3c</b> (%CV)
1	100 (2.8)	100 (1.0)	100 (1.8)	100 (2.5)
8	96 (2.3)	98 (3.6)	94 (3.3)	97 (1.1)
17	96 (3.8)	96 (3.3)	94 (2.6)	95 (2.9)
23	89 (1.8)	95 (4.1)	89 (3.2)	91 (2.7)
30	89 (2.1)	92 (2.7)	89 (3.6)	87 (2.7)

## Conclusions

We have described the syntheses of three new acridinium esters with conjugation sites at the acridinium nitrogen using a simple and general synthetic protocol starting from easily synthesized *N*-sulfopropylacridinium esters. In this study, we have provided the first direct comparison of the properties of chemiluminescent acridinium dimethylphenyl esters with different conjugation sites, one where the light emitting acridone moiety is cleaved from its conjugate partner (conventional labeling) and another where the acridone remains attached to the conjugate. Our results show that the conjugation at the acridinium nitrogen, which also alters how the acridinium ring and phenol are oriented with respect to the protein surface, has a minimal impact on emission kinetics and emission spectra. However, this mode of conjugation to three different proteins was observed to significantly increase light yield which should be useful for improving the immunoassay sensitivity. How orientation of the acridinium ester molecule on the protein surface affects non-specific binding and the actual immunoassay performance are areas for further investigation.

## Experimental

### General

Chemicals were purchased from Sigma-Aldrich (Milwaukee, Wisconsin, USA) unless indicated otherwise. All the final acridinium esters, intermediates and reaction mixtures were analyzed and/or purified by HPLC using a Beckman-Coulter HPLC system. For analytical HPLC, either a Phenomenex, Kinetex, C<sub>18</sub>, 2.6 micron, 4.6 × 50 mm column or a Phenomenex C<sub>18</sub>,

10 micron, 3.9 × 300 mm column were used with MeCN–water (each with 0.5% trifluoroacetic acid, TFA) as the solvents at a flow rate of 1 mL minute<sup>−1</sup> and UV detection at 260 nm. Preparative HPLC was performed using a Phenomenex, Luna C<sub>18</sub>, 5 micron, 30 × 250 mm column at a flow rate of 20 mL minute<sup>−1</sup> and UV detection at 260 nm. MALDI-TOF (Matrix-Assisted Laser Desorption Ionization-Time of Flight) mass spectroscopy was performed using a VOYAGER DE Biospectrometry Workstation from ABI. This is a bench top instrument operating in the linear mode with a 1.2 meter ion path length, flight tube. Spectra were acquired in positive ion mode. For small molecules, α-cyano-4-hydroxycinnamic acid was used as the matrix and spectra were acquired with an accelerating voltage of 20 000 volts and a delay time of 100 ns. For protein conjugates, sinapinic acid was used as the matrix and spectra were acquired with an accelerating voltage of 25 000 volts and a delay time of 85 ns.

For HRMS (High Resolution Mass Spectra), samples were dissolved in HPLC-grade methanol and analyzed by direct-flow injection (injection volume = 5 μL) ElectroSpray Ionization (ESI) on a Waters Qtof API US instrument in the positive ion mode. Optimized conditions are as follows: capillary = 3000 kV, cone = 35, source temperature = 120 °C, desolvation temperature = 350 °C.

NMR spectra (proton and carbon) were recorded on a Bruker 600 MHz spectrometer. To suppress pseudobase formation, spectra of the acridinium esters and intermediates were acquired in an acidic solvent, namely deuterated trifluoroacetic acid so that two forms of the compounds were not present during spectral analysis. Chemiluminescence measurements were carried out using a Berthold Technologies' AutoLumat Plus LB 953 luminometer. Emission spectra were recorded in >90% aqueous media using a PR-740 spectroradiometer (camera) from Photo Research Inc. Bandwidth slit: 2 nm; aperture: 0.5–2 degrees; exposure time: 5000 ms.

### Synthesis of acridinium esters (Fig. 3)

**Compound 2a.** A solution of compound **1** (50 mg, 0.07 mmole) in 1 : 1 DMF–MeCN (6 mL) was treated with compound **i** (Aldrich, 0.051 mL, 5 equivalents). The reaction was heated at 75 °C in an oil bath under a nitrogen atmosphere for 1 hour. HPLC analysis using a Phenomenex, C<sub>18</sub>, 10 micron, 3.9 × 300 mm column and a 30 minute gradient of 10 → 100% MeCN–water (each with 0.05% TFA) at a flow rate of 1 mL minute<sup>−1</sup> and UV detection at 260 nm showed clean conversion to product **2a** eluting at 16.5 minutes. The product was purified by preparative HPLC using the same gradient and the HPLC fractions were frozen at −80 °C and lyophilized to dryness. Yield = 34 mg (71%). <sup>1</sup>H-NMR (CF<sub>3</sub>COOD) 1.58 (d, 6H, *J* = 6.1 Hz), 2.61 (s, 6H), 2.92 (m, 2H), 3.57 (brt, 2H), 3.62 (brt, 2H), 3.81 (brt, 2H), 3.93–4.03 (m, 8H), 4.14 (s, 3H), 4.98 (spt, 1H, *J* = 6.1 Hz), 5.77 (brt, 2H), 7.94 (d, 1H, *J* = 2.6 Hz), 8.06 (s, 2H), 8.16 (dd, 1H, *J* = 8.8, 6.8 Hz), 8.26 (m, 1H), 8.50 (m, 1H), 8.72 (brd, 2H), 8.79 (d, 1H, *J* = 8.8 Hz); <sup>13</sup>C-NMR (CF<sub>3</sub>COOD) 18.55, 18.76, 22.20, 22.23, 24.84, 42.77, 44.43, 51.68, 51.85, 55.11, 67.98, 71.79, 72.17, 75.28, 75.40, 107.16, 119.88, 121.63,

126.27, 128.22, 130.06, 130.72, 131.86, 133.23, 133.50, 138.90, 140.45, 141.14, 141.53, 147.65, 154.26, 160.98, 165.79, 172.25; MALDI-TOF MS  $m/z$  696.9  $M^+$ ; HRMS  $m/z$  696.2964  $M^+$  (696.2955 calculated).

**Compound 2b.** A solution of compound **1** (50 mg, 0.07 mmole) in 1 : 1 DMF–MeCN (6 mL) was treated with compound **ii** (0.1 g, 5 equivalents). The reaction was heated at 75 °C in an oil bath under a nitrogen atmosphere for 1 hour. HPLC analysis as described above showed clean conversion to product **2b** eluting at 17.0 minutes. The product was purified by preparative HPLC using the same gradient and the HPLC fractions were frozen at –80 °C and lyophilized to dryness. Yield = 36 mg (64%).  $^1\text{H-NMR}$  ( $\text{CF}_3\text{COOD}$ ) 1.59 (d, 6H,  $J$  = 6.1 Hz), 2.62 (s, 6H), 2.95 (m, 2H), 3.56 (brt, 2H), 3.64 (brt, 2H), 3.84 (brt, 2H), 3.97 (m, 18H), 4.03 (m, 2H), 4.15 (s, 3H), 4.99 (spt, 1H,  $J$  = 6.1 Hz), 5.80 (brt, 2H), 7.95 (d, 1H,  $J$  = 2.5 Hz), 8.08 (s, 2H), 8.17 (dd, 1H,  $J$  = 8.8, 6.8 Hz), 8.28 (dd, 1H,  $J$  = 9.9, 2.6 Hz), 8.48–8.54 (m, 1H), 8.75 (brd, 2H), 8.80 (d, 1H,  $J$  = 8.8);  $^{13}\text{C-NMR}$  ( $\text{CF}_3\text{COOD}$ ) 18.55, 18.75, 22.20, 22.22, 24.82, 42.52, 44.45, 51.63, 51.87, 55.08, 68.21, 71.74, 71.82, 72.10, 72.36, 75.26, 75.39, 107.15, 119.90, 121.65, 126.26, 128.20, 130.04, 130.71, 131.85, 133.22, 133.49, 138.87, 140.46, 141.11, 141.54, 147.60, 154.24, 160.96, 165.80, 172.26; MALDI-TOF MS  $m/z$  828.9  $M^+$ ; HRMS  $m/z$  828.3731  $M^+$  (828.3741 calculated).

**Compound 2c.** A solution of compound **1** (50 mg, 0.07 mmole) in DMSO (6 mL) was treated with compound **iii** (0.15 g, HBr salt, 5 equivalents) and diisopropylethylamine (0.12 mL, 10 equivalents). The reaction was heated at 75 °C in an oil bath under a nitrogen atmosphere for 1 hour. HPLC analysis as described above showed clean conversion to product **2b** eluting at 15.0 minutes. The product was purified by preparative HPLC using the same gradient and the HPLC fractions were frozen at –80 °C and lyophilized to dryness. Yield = 29 mg (52%).  $^1\text{H-NMR}$  ( $\text{CF}_3\text{COOD}$ ) 1.61 (d, 6H,  $J$  = 6.1 Hz), 2.35 (m, 2H), 2.64 (m, 10H), 2.95 (m, 2H), 3.30 (s, 3H), 3.50 (brt, 2H), 3.54 (brt, 2H), 3.58 (brt, 2H), 3.68–3.79 (m, 4H), 3.83 (brt, 2H), 3.85–3.91 (m, 2H), 4.17 (s, 3 H), 5.00 (spt, 1H,  $J$  = 6.1 Hz), 5.80 (brt, 2H), 7.97 (d, 1H,  $J$  = 2.5 Hz), 8.09 (s, 2H), 8.19 (dd, 1 H,  $J$  = 8.8, 6.8 Hz), 8.30 (m, 1H), 8.53 (m, 1H), 8.74 (brd, 2H), 8.82 (d, 1H,  $J$  = 8.7 Hz);  $^{13}\text{C-NMR}$  ( $\text{CF}_3\text{COOD}$ ) 18.55, 18.76, 20.07, 22.20, 22.23, 22.67, 24.76, 25.32, 40.16, 42.06, 49.76, 51.36, 51.83, 55.10, 61.46, 62.48, 62.68, 75.29, 75.41, 107.23, 119.85, 121.58, 126.27, 128.21, 130.06, 130.72, 131.87, 133.23, 133.50, 138.89, 140.43, 141.18, 141.53, 147.65, 154.24, 160.99, 165.77, 172.25; MALDI-TOF MS  $m/z$  816.1  $M^+$ ; HRMS  $m/z$  815.3387  $M^+$  (815.3360 calculated).

**Compound 3a.** A solution of compound **2a** (8 mg, 0.011 mmole) in acetonitrile (1 mL) was mixed with 0.1 M sodium phosphate pH = 7.2 (1 mL) and disuccinimidyl glutarate (DSG, 37.5 mg, 10 equivalents) was added. The reaction was stirred at room temperature for 1 hour. HPLC analysis using a Phenomenex, Kinetex  $\text{C}_{18}$ , 2.6 micron, 4.6 × 50 mm column and a 10 minute gradient of 10 → 90% MeCN–water (each with 0.05% TFA) at a flow rate of 1 mL minute<sup>–1</sup> and UV detection at 260 nm showed clean conversion to product **3a**

eluting at 7.3 minutes. The product was purified by preparative HPLC using a Phenomenex, Luna  $\text{C}_{18}$ , 5 micron, 30 × 250 mm column and a 30 minute gradient of 10 → 90% MeCN–water (each with 0.05% TFA) at a flow rate of 20 mL minute<sup>–1</sup> and UV detection at 260 nm. HPLC fractions containing the product were frozen at –80 °C and lyophilized to dryness. Yield = 6.4 mg (61%).  $^1\text{H-NMR}$  ( $\text{CF}_3\text{COOD}$ ) 1.54 (d, 6H,  $J$  = 6.1 Hz), 2.25 (m, 2H), 2.57 (s, 6H), 2.77 (brt, 2H), 2.84 (brt, 2H), 2.86–2.94 (m, 2H), 3.06 (s, 4H), 3.59 (t, 2H,  $J$  = 5.1 Hz), 3.78 (m, 4H), 3.90–4.00 (m, 8H), 4.10 (s, 3H), 4.94 (spt, 1H,  $J$  = Hz), 5.75 (brt, 2H), 7.90 (d, 1H,  $J$  = 2.6 Hz), 8.02 (s, 2H), 8.12 (m, 1H), 8.23 (m, 1H), 8.46 (m, 1H), 8.70 (brd, 2H), 8.75 (brd, 1H);  $^{13}\text{C-NMR}$  ( $\text{CF}_3\text{COOD}$ ) 18.52, 18.72, 22.16, 22.19, 24.78, 26.90, 27.24, 31.43, 35.61, 42.93, 44.40, 51.62, 51.84, 70.77, 71.84, 72.33, 75.24, 75.36, 107.12, 119.85, 121.59, 126.23, 127.28, 128.18, 130.01, 130.69, 131.82, 133.18, 133.46, 138.85, 140.43, 141.08, 141.50, 147.59, 154.20, 160.94, 165.76, 171.13, 172.22, 176.15, 178.98; MALDI-TOF MS  $m/z$  907.1  $M^+$ ; HRMS  $m/z$  907.3459  $M^+$  (907.3435 calculated).

**Compound 3b.** A solution of compound **2b** (10 mg, 0.012 mmole) in acetonitrile (2.5 mL) was mixed with 0.1 M sodium phosphate pH = 7.2 (1 mL) and DSG (39.5 mg, 10 equivalents) was added. The reaction was stirred at room temperature for 1 hour. HPLC analysis as described above showed clean conversion to product **3b** eluting at 7.3 minutes. The product was purified by preparative HPLC using a 30 minute gradient of 10 → 70% MeCN–water (each with 0.05% TFA) and the HPLC fraction was frozen at –80 °C and lyophilized to dryness. Yield = 6.3 mg (50%).  $^1\text{H-NMR}$  ( $\text{CF}_3\text{COOD}$ ) 1.55 (d, 6H,  $J$  = 6.1 Hz), 2.26 (m, 2H), 2.58 (s, 6H), 2.80 (brt, 2H), 2.86 (brt, 2H), 2.88–2.95 (m, 2H), 3.08 (s, 4H), 3.60 (brt, 2H), 3.70–3.80 (m, 4H), 3.90–4.00 (m, 20H), 4.11 (s, 3H), 4.95 (spt, 1H,  $J$  = 6.1 Hz), 5.76 (brt, 2H), 7.91 (d, 1H,  $J$  = 2.3 Hz), 8.04 (s, 2H), 8.13 (m, 1H), 8.24 (m, 1H), 8.48 (m, 1H), 8.71 (brd, 2H), 8.77 (d, 1H,  $J$  = 8.6 Hz);  $^{13}\text{C-NMR}$  ( $\text{CF}_3\text{COOD}$ ) 18.54, 18.74, 22.19, 22.23, 22.43, 24.83, 26.94, 27.26, 31.43, 35.41, 35.46, 43.24, 44.42, 51.66, 51.87, 55.16, 71.60, 71.88, 72.10, 72.42, 75.27, 75.38, 107.14, 119.89, 121.63, 126.26, 128.20, 130.04, 130.72, 131.85, 133.21, 133.49, 133.88, 140.46, 141.11, 141.53, 147.61, 154.22, 160.96, 165.78, 171.08, 172.24, 176.18, 179.00; MALDI-TOF MS  $m/z$  1039.2  $M^+$ ; HRMS  $m/z$  1039.4260  $M^+$  (1039.4222 calculated).

**Compound 3c.** A solution of compound **2c** (9 mg, 0.011 mmole) in acetonitrile (1.5 mL) was mixed with 0.1 M sodium phosphate pH = 7.2 (1 mL) and DSG (40 mg, 11 equivalents) was added. The reaction was stirred at room temperature for 1 hour. HPLC analysis as described above showed 80% conversion to product **3c** eluting at 6.4 minutes. The product was purified by preparative HPLC using a 40 minute gradient of 10 → 60% MeCN–water (each with 0.05% TFA) and the HPLC fraction was frozen at –80 °C and lyophilized to dryness. Yield = 7.5 mg (66%).  $^1\text{H-NMR}$  ( $\text{CF}_3\text{COOD}$ ) 1.55 (d, 6H,  $J$  = 6.1 Hz), 2.21 (m, 2H), 2.24–2.34 (m, 4H), 2.53–2.60 (m, 8H), 2.65 (m, 2H), 2.82 (t, 2H,  $J$  = 6.8 Hz), 2.89 (m, 2H), 3.08 (s, 4H), 3.21 (s, 3H), 3.44 (m, 2H), 3.48–3.56 (m, 4H), 3.58 (brt, 2H), 3.61–3.71 (m, 2H), 3.77 (m, 4H), 4.11 (s, 3H), 4.95 (spt, 1H,  $J$  =

6.0 Hz), 5.75 (brt, 2H), 7.91 (d, 1H,  $J = 2.6$  Hz), 8.03 (s, 2H), 8.13 (m, 1H), 8.25 (m, 1H), 8.48 (m, 1H), 8.69 (brd, 2H), 8.76 (brd, 1H);  $^{13}\text{C}$ -NMR ( $\text{CF}_3\text{COOD}$ ) 18.46, 18.66, 22.11, 22.14, 22.40, 26.86, 27.20, 31.46, 39.45, 42.04, 49.67, 50.37, 50.71, 51.33, 51.75, 55.01, 61.98, 62.26, 75.20, 75.31, 107.12, 119.77, 121.51, 126.17, 128.12, 129.96, 130.63, 131.78, 133.13, 133.40, 138.81, 140.35, 141.09, 141.44, 147.56, 154.15, 160.89, 165.69, 171.17, 172.16, 176.16, 178.92; MALDI-TOF MS  $m/z$  1026.6  $\text{M}^+$ ; HRMS  $m/z$  1026.3817  $\text{M}^+$  (1026.3840 calculated).

### Synthesis of protein conjugates of acridinium esters (Table 1)

The following procedure illustrated for labeling of BSA was used for labeling the anti-TSH and anti-HBsAg antibodies as well.

BSA (1 mg, 15 nanomoles, 0.2 mL of a 5  $\text{mg mL}^{-1}$  solution) was diluted with 0.2 mL of 0.1 M sodium carbonate, pH 9. The protein solutions, in separate labeling reactions, were treated with ten equivalents of various acridinium esters **3a–3c** and **4**. The acridinium esters were dissolved in dimethyl sulfoxide to give 5  $\text{mg mL}^{-1}$  solutions. For labeling with the various acridinium esters, 0.0302 mL of **4**, 0.0274 mL of **3a**, 0.0314 mL of **3b** and 0.0309 mL of **3c** were added. The reactions were stirred at room temperature for 2–3 hours. The reactions were then diluted with 0.5 mL de-ionized water and transferred to 4 mL Amicon filters from Millipore (MW 30 000 cutoff). The labeling reactions in the filters were further diluted with 3 mL de-ionized water. The solutions were concentrated to  $\sim 0.1$  mL by centrifugation at 3500g for 10 minutes. This dilution and concentration process was repeated three more times. The final conjugate solutions were transferred to vials and the solutions were frozen and lyophilized. The lyophilized conjugates were dissolved in de-ionized water to give  $\sim 2$   $\text{mg mL}^{-1}$  solutions (protein assay). The conjugates were analyzed by MALDI-TOF mass spectrometry to measure acridinium ester incorporation. This entailed measuring the molecular weight of the unlabeled protein and the labeled protein. The acridinium ester label contributed to the observed difference in mass between these two measurements. By knowing the molecular weight of the specific acridinium ester label, the extent of label incorporation for that specific acridinium ester could thus be calculated (Table 1).

### Chemiluminescence measurements (Fig. 4, 6, S7–S10 ESI†)

The chemiluminescence of free labels and protein conjugates of acridinium esters (Fig. 3) was measured on an Autolumat LB953 Plus luminometer from Berthold Technologies. Free labels, amine derivative of **4** and **2a–2c**, were dissolved in DMSO to give 0.2–0.5 mM solutions. These solutions were serially diluted  $10^6$ -fold for chemiluminescence measurements in an aqueous buffer of 10 mM disodium hydrogen phosphate, 0.15 M NaCl, 8 mM sodium azide and 0.015 mM bovine serum albumin (BSA), pH = 8.0. Protein conjugates,  $\sim 2$   $\text{mg mL}^{-1}$ , were serially diluted  $10^5$ -fold for chemiluminescence measurements in the same buffer. A 0.010 mL volume of each diluted acridinium ester or conjugate sample was dispensed into the

bottom of a cuvette. Cuvettes were placed into the primed LB953 and the chemiluminescence reaction was initiated with the sequential addition of 0.3 mL of reagent 1, a solution of 0.5% hydrogen peroxide in 0.1 M nitric acid followed by the addition of 0.3 mL of reagent 2, a solution of 0.25 M sodium hydroxide with or without a surfactant. For measurements with CTAC, 7 mM of this cationic surfactant was included in reagent 2.

Each chemiluminescence flash curve was measured in 100 intervals of 0.1 second (10 seconds total time, CTAC) or 240 intervals of 0.5 seconds (2 minutes total time, no surfactant) from the point of chemiluminescence initiation with the addition of 0.25 M NaOH. Each chemiluminescence reaction was carried out a minimum of three times, averaged and converted to a percentage of the chemiluminescence accumulated up to each time interval. The output from the luminometer instrument was expressed as R.L.U.s (Relative Light Units).

### Emission wavelength measurements (Fig. 5, S11 and S12)

Visible wavelength emission spectra of the acridinium esters **4** (amine derivative), **2a–2c** and the protein conjugates of **4**, **3a–3c** were measured by FSSS (Fast Spectral Scanning System) using a PR-740 spectroradiometer (camera) from Photo Research Inc. The following instrument parameters were used: bandwidth slit: 2 nm; aperture: 0.5–2 degrees; exposure time: 5000 ms. In a typical measurement, 0.01 mL of a 5  $\text{mg mL}^{-1}$  solution of the acridinium ester in DMSO or 0.025–0.05 mL of the protein conjugates at 2  $\text{mg mL}^{-1}$  were diluted with 0.3 mL of reagent 1 comprising 0.5% hydrogen peroxide in 0.1 M nitric acid. Just prior to the addition of reagent 2 comprising 7 mM CTAC in 0.25 M sodium hydroxide, the shutter of the camera was opened and light was collected for 5 seconds. The output of the instrument is a graph of light intensity *versus* wavelength.

### Chemiluminescence stability measurements (Tables 3 and 4)

The acridinium ester labeled BSA conjugates were diluted to a concentration of 0.2 nM in an aqueous buffer of 10 mM phosphate, 0.15 M NaCl, 8 mM sodium azide and 0.015 mM bovine serum albumin (BSA), pH = 6.0 or 7.4. Two milliliter volumes of the diluted conjugates were sealed in glass vials and incubated at 25 °C for 30 days protected from light. Chemiluminescence of 0.01 mL samples (five replicates) of the diluted conjugates was periodically measured as a function of time. Chemiluminescence was measured on a Berthold Technologies' AutoLumat Plus LB953 luminometer. The averaged results were calculated as residual chemiluminescence percentages with respect to values determined at day 1.

## Acknowledgements

We thank Mr Richard Wright for NMR spectra and Dr Shenliang Wang for assistance with emission spectrum measurements.

## References

- 1 (a) S.-J. Law, C. S. Leventis, A. Natrajan, Q. Jiang, P. B. Connolly, J. P. Kilroy, C. R. McCudden and S. M. Tirrell, *US Pat.* 5,656,426, 1997; (b) A. Natrajan, D. Sharpe and Q. Jiang, *US Pat.* 6,664,043 B2, 2003; (c) A. Natrajan, Q. Jiang, D. Sharpe and J. Costello, *US Pat.*, 7,309,615, 2007; (d) A. Natrajan, D. Sharpe, J. Costello and Q. Jiang, *Anal. Biochem.*, 2010, **406**, 204–213; (e) A. Natrajan, D. Sharpe and D. Wen, *Org. Biomol. Chem.*, 2011, **9**, 5092–5103; (f) A. Natrajan, D. Sharpe and D. Wen, *Org. Biomol. Chem.*, 2012, **10**, 1883–1895; (g) A. Natrajan, D. Sharpe and D. Wen, *Org. Biomol. Chem.*, 2012, **10**, 3432–3447; (h) A. Natrajan and D. Sharpe, *Org. Biomol. Chem.*, 2013, **11**, 1026–1039; (i) A. Natrajan, D. Wen and D. Sharpe, *Org. Biomol. Chem.*, 2014, **12**, 3887–3901; (j) A. Natrajan and D. Wen, *RSC Adv.*, 2014, **4**, 21852–21863.
- 2 (a) I. Weeks, I. Behesti, F. McCapra, A. K. Campbell and J. S. Woodhead, *Clin. Chem.*, 1983, **29/8**, 1474–1479; (b) J. W. Bunting, V. S. F. Chew, S. B. Abhyankar and Y. Goda, *Can. J. Chem.*, 1984, **62**, 351–354; (c) P. W. Hammond, W. A. Wiese, A. A. Waldrop III, N. C. Nelson and L. J. Arnold Jr., *J. Biolumin. Chemilumin.*, 1991, **6**, 35–43.
- 3 (a) P. D. Profio, R. Germani, G. Savelli, G. Cerichelli, N. Spreti and C. A. Bunton, *J. Chem. Soc., Perkin Trans. 2*, 1996, 1505–1509; (b) G. Cerichelli, L. Luchetti, G. Mancini, M. N. Muzzioli, R. Germani, P. P. Ponti, N. Spreti, G. Savelli and C. A. Bunton, *J. Chem. Soc., Perkin Trans. 2*, 1989, 1081–1085; (c) G. Cerichelli, G. Mancini, L. Luchetti, G. Savelli and C. A. Bunton, *J. Phys. Org. Chem.*, 1991, **4**, 71–76; (d) G. Cerichelli, L. Luchetti, G. Mancini, G. Savelli and C. A. Bunton, *Langmuir*, 1996, **12**, 2348–2352; (e) L. Brinchi, P. D. Profio, R. Germani, G. Savelli and C. A. Bunton, *Langmuir*, 1997, **13**, 4583–4587; (f) L. Brinchi, R. Germani, G. Savelli, N. Spreti, R. Ruzziconi and C. A. Bunton, *Langmuir*, 1998, **14**, 2656–2662; (g) L. Brinchi, R. Germani, G. Savelli and C. A. Bunton, *J. Phys. Org. Chem.*, 1999, **12**, 890–894.
- 4 (a) F. McCapra, *Acc. Chem. Res.*, 1976, **9/6**, 201–208; (b) F. McCapra, D. Watmore, F. Sumun, A. Patel, I. Beheshti, K. Ramakrishnan and J. Branson, *J. Biolumin. Chemilumin.*, 1989, **4**, 51–58; (c) J. Rak, P. Skurski and J. Błażejowski, *J. Org. Chem.*, 1999, **64**, 3002–3008; (d) K. Krzyminiński, A. D. Roshal, B. Zadykowicz, A. Białk-Bielińska and A. Sieradzan, *J. Phys. Chem. A*, 2010, **114**, 10550–10562; (e) K. Krzyminiński, A. Ożóg, P. Malecha, A. D. Roshal, A. Wróblewska, B. Zadykowicz and J. Błażejowski, *J. Org. Chem.*, 2011, **76**, 1072–1085.
- 5 (a) I. Weeks, A. K. Campbell and J. S. Woodhead, *Clin. Chem.*, 1983, **29/8**, 1480–1483; (b) S.-J. Law, T. Miller, U. Piran, C. Klukas, S. Chang and J. Unger, *J. Biolumin. Chemilumin.*, 1989, **4**, 88–98; (c) N. C. Nelson, A. B. Cheikh, E. Matsuda and M. M. Beckyer, *Biochemistry*, 1996, **35**, 8429–8438; (d) L. J. Kricka, *Anal. Chim. Acta*, 2003, **500**, 279–286.
- 6 (a) Q. Jiang, J. Xi, A. Natrajan, D. Sharpe, M. Baumann, R. Hilfiker, E. Schmidt, P. Senn, F. Thommen, A. Waldner, A. Alder and S.-J. Law, *US Pat.* 6,165,800, 2000; (b) A. Natrajan, T. Sells, H. Schroeder, G. Yang, D. Sharpe, Q. Jiang, H. Lukinsky and S.-J. Law, *US Pat.* 7,319,041, 2008.
- 7 (a) G. Zomer and J. F. C. Stavenuiter, *Anal. Chim. Acta*, 1989, **227**, 11–19; (b) S. Batmanghelich, J. S. Woodhead, K. Smith and I. Weeks, *J. Photochem. Photobiol., A*, 1991, **56**, 249–254.
- 8 (a) N. Sato, *Tetrahedron Lett.*, 1996, **47**, 8519–8522; (b) M. Adamczyk, P. G. Mattingly, J. A. Moore and Y. Pan, *Org. Lett.*, 2003, **5**, 3779–3782.
- 9 (a) R. C. Brown, Z. Li, A. J. Rutter, X. Mu, O. H. Weeks, K. Smith and I. Weeks, *Org. Biomol. Chem.*, 2009, **7**, 386–394; (b) K. A. Browne, D. D. Deheyn, G. A. El-Hiti, K. Smith and I. Weeks, *J. Am. Chem. Soc.*, 2011, **133**, 14637–14648; (c) K. A. Browne, D. D. Deheyn, R. C. Brown and I. Weeks, *Anal. Chem.*, 2012, **84**, 9222–9229.
- 10 A. Natrajan and D. Wen, *Green Chem.*, 2011, **13**, 913–921.
- 11 D. C. Carter and J. X. Ho, *Adv. Protein Chem.*, 1994, **45**, 153–203.
- 12 (a) W. L. Hinze, T. E. Riehl and H. N. Singh, *Anal. Chem.*, 1984, **56**, 2180–2191; (b) M. Siegmund and J. Bendig, *Ber. Bunsen-Ges. Phys. Chem.*, 1978, **82**, 1061–1068; (c) M. Siegmund and J. Bendig, *Z. Naturforsch., A: Phys. Phys. Chem. Kosmophys.*, 1980, **35**, 1076–1086; (d) S. Mory, H.-J. Weigman, A. Rosenfeld, M. Siegmund, R. Mitzner and J. Bendig, *Chem. Phys. Lett.*, 1985, **115**, 201–204.